HHS Public Access

Author manuscript

J Endocrinol. Author manuscript; available in PMC 2022 May 24.

Published in final edited form as:

J Endocrinol. ; 249(3): 223–237. doi:10.1530/JOE-21-0009.

Role of ERβ in adipocyte metabolic response to wheel running following ovariectomy

Laura M Clart[1], **Rebecca J Welly**[1], **Eric D Queathem**[1], **R Scott Rector**[1,2,3], **Jaume Padilla**[1,4], **Christopher P Baines**[5], **Jill A Kanaley**[1], **Dennis B Lubahn**[6], **Victoria J Vieira-Potter**[1]

[1]Department of Nutrition and Exercise Physiology, University of Missouri System, Columbia, Missouri, USA

[2]Internal Medicine-Division of Gastroenterology and Hepatology, University of Missouri System, Columbia, Missouri, USA

[3]Research Service, Truman VA Memorial Hospital, Columbia, Missouri, USA

[4]Dalton Cardiovascular Research Center, University of Missouri System System, Columbia, Missouri, USA

[5]Department of Biomedical Sciences, University of Missouri System, Columbia, Missouri, USA

[6]Department of Biochemistry, University of Missouri System, Columbia, Missouri, USA

Abstract

Estrogen receptor β (ERb), one of the two major estrogen receptors, acts via genomic and non-genomic signaling pathways to affect many metabolic functions, including mitochondrial biogenesis and respiration. This study assessed the effect of ERb classical genomic activity on adipocyte-specific and -systemic metabolic responses to wheel running exercise in a rodent model of menopause. Female mice lacking the ERb DNA-binding domain ($ERb_{DBD}KO$, $n = 20$) and WT ($n = 21$) littermate controls were fed a high-fat diet (HFD), ovariectomized (OVX), and randomized to control (no running wheel) and exercise (running wheel access) groups and were followed for 8 weeks. Wheel running did not confer protection against metabolic dysfunction associated with HFD+OVX in either $ERb_{DBD}KO$ or WT mice, despite increased energy expenditure. Unexpectedly, in the $ERb_{DBD}KO$ group, wheel running increased fasting insulin and surrogate measures of insulin resistance, and modestly increased adipose tissue inflammatory gene expression ($P \leq 0.05$). These changes were not accompanied by significant changes in adipocyte mitochondrial respiration. It was demonstrated for the first time that female WT OVX mice do experience exercise-induced browning of white adipose tissue, indicated by a robust increase in uncoupling protein 1 (UCP1) ($P \leq 0.05$). However, KO mice were completely resistant to this effect, indicating that full ERb genomic activity is required for exercise-induced browning. The inability to upregulate UCP1 with exercise following OVX may have resulted in the increased insulin resistance observed in KO mice, a hypothesis requiring further investigation.

Correspondence should be addressed to V J Vieira-Potter: vieirapotterv@missouri.edu.

Declaration of interest

The authors declare that there is no conflict of interest that could be perceived as prejudicing the impartiality of the reported research.

Keywords

estrogen receptor beta; DNA-binding domain; ovariectomy; adipose tissue

Introduction

Estradiol (E_2), the most abundant form of circulating estrogens in premenopausal women, exerts many beneficial effects, protecting women from various cardiovascular and metabolic diseases (Wake & Yoshiyama 2009, Kautzky-Willer *et al.* 2016). This protection is lost when women reach menopause, resulting in significant increases in body weight, insulin resistance, and dyslipidemia (Kozakowski *et al.* 2017).

Estrogen receptor α (ERa) and β (ERb) are nuclear transcription factors that regulate the expression of target genes which influence many pathways that elicit cardiovascular protection, cell survival, and mitochondrial function (Klinge 2008). They function via genomic or non-genomic pathways. The genomic or 'classical' pathway involves the dimerization of receptor and E_2 and translocation to the nucleus, where the receptor binds to E_2 response elements (EREs), resulting in gene transcription. By contrast, the non-genomic or 'rapid' pathway involves the binding of E_2 to receptors located on cell membranes, in the cytoplasm, or mitochondria, leading to the activation of signal transduction pathways. These pathways may indirectly also affect the gene regulation via their activation of other transcription factors (Deroo & Korach 2006, Madak-Erdogan *et al.* 2008). While both receptors are present in adipose tissue, compared to ERa, much less is known about the adipose tissue-specific effects of ERb. In terms of its metabolic effects, ERb has been shown to enhance pancreatic beta-cell insulin release (Soriano *et al.* 2009), has anti-obesity effects (Yepuru *et al.* 2010) and increases mitochondrial biogenesis (Liao *et al.* 2015). Importantly, both ERa and ERb localize to the mitochondria. The presence of ERb within the mitochondria is of particular relevance, as previous studies have demonstrated that ERb ligands increase adipose tissue mitochondrial activity (Ponnusamy *et al.* 2017).

Postmenopausal women (and ovariectomized (OVX) rodents) develop obesity resulting in dysfunctional white adipose tissue (WAT), which is characterized by increased inflammation and reduced insulin responsiveness. Importantly, dysfunctional WAT contributes to the development of cardiovascular disease and insulin resistance. Mitochondrial dysfunction in adipose tissue may be mechanistically related to that dysfunctional phenotype (Kusminski & Scherer 2012). While WAT has a very low mitochondrial density relative to other tissues, a healthier adipose tissue is characterized by greater adipocyte mitochondrial density and function. In a process termed 'browning' WAT becomes more like mitochondria-dense brown adipose tissue (BAT) (Giralt & Villarroya 2013). Moreover, compared to traditional WAT, this 'beige' adipose tissue is more insulin sensitive and less inflamed and thus, improves systemic metabolic health. Exercise is known to improve adipose tissue function and has been shown to induce browning (Stallknecht *et al.* 1991, Otero-Díaz *et al.* 2018, Stanford *et al.* 2015). For unknown reasons, not all studies have confirmed this (Aldiss *et al.* 2019). Thus, why some but not all rodents and humans are prone to exercise-induced browning (i.e. the mechanism) is not known and remains a critical unanswered question.

Pharmacological activation of ERb has been shown to increase adipocyte mitochondrial function in mice and significantly upregulate uncoupling protein 1 (UCP1), the signature protein in beige and BAT (Ponnusamy *et al.* 2017). Interestingly, in addition to confirming that exercise induces adipocyte mitochondrial activity and UCP1 expression, our group recently demonstrated that exercise also significantly upregulates ERb expression in WAT (Winn *et al.* 2019). Together, these findings suggest that ERb may be involved in the browning process. Considering the known localization of ERb to the mitochondria and recently identified effects on adipocyte mitochondria combined with our recent discoveries that: (1) exercise increases ERb expression in WAT (Winn *et al.* 2019); (2) unopposed signaling through ERb increases sensitivity to WAT browning (Clookey *et al.* 2019) and (3) lack of ERb exacerbates the negative WAT responses to OVX (Zidon *et al.* 2020), we tested the hypothesis that ERb is required for optimal exercise-induced WAT and systemic metabolic effects following ovarian hormone loss. Thus, we determined how lack of the ERb DNA-binding domain (ERbDBD) (i.e. elimination of classical genomic signaling of ERb) would affect exercise-mediated UCP1 increase in WAT and the associated systemic responses to exercise. We predicted that mice lacking the ERb DBD would display suppressed adipocyte mitochondrial function and be resistant to exercise-mediated adipose and systemic metabolic improvements. While we found that voluntary wheel running was not sufficient to counter OVX-induced metabolic dysfunction, we found unexpectedly that the KO mice responded adversely to wheel running by increasing insulin resistance. Remarkably, this coincided with complete resistance to exercise-induced UCP1 upregulation, implicating ERb genomic activity as being essential for exercise-mediated beigeing, at least in rodents following OVX.

Methods

Ethical approval

All animal husbandry and experimental procedures were carried out in accordance with AAALAC International and approved by the University of Missouri Institutional Animal Care and Use Committee.

Mouse model

The mice were provided by Dennis Lubahn, an author of this study, who generated and bred the mice as described in Krege *et al.* (1998). He also oversaw the genotyping and validation of the mouse model. These mice are not classical whole-body ERb knockouts. Instead, their ERbDBD has been knocked out (i.e. $ERb_{DBD}KO$) via a neo cassette interrupting the translation of the gene at the DBD, at exon 3 (Krege *et al.* 1998). This presents an opportunity to investigate the effects of the absence of this domain, while maintaining other functions of this receptor, including its mitochondrial and non-classical genomic effects.

Study design

Female $ERB_{DBD}KO$ (KO) ($n = 34$) and littermate control (i.e. WT) mice ($n = 32$) were housed under thermoneutral conditions (26–28°C) and kept at 12 h light:12 h darkness cycle (light cycle from 07:00 h to 19:00 h). Beginning at ~11 (range 10.5–11.5) weeks of age, mice were provided, for 5 weeks, a high-fat diet (HFD) *ad libitum*(46.4% fat:36.0%

carbohydrate:17.6% protein) (Test Diet, St. Louis, MO, #1814692) prior to the intervention mice being ovariectomized. A subset of WT (n = 11) and KO (n = 14) was left ovary-intact as a comparison to assess and compare the effects of ovariectomy, on WT and KO mice. None of these ovary-intact mice were provided running wheels. Prior to surgery, the mice were housed in pairs; after ovariectomy, they were individually housed. Intervention mice were ovariectomized at 15.5–16.5 weeks of age and given 2 weeks to recover post-surgery before the exercise groups were provided running wheels. Next, half of the mice were provided a running wheel for 8 weeks (n = 10 KOEx; 10 WTEx) while the other half did not have access to running wheels (n = 10 KOCon; 11 WTCon). After 8 weeks, the tissues were harvested. Before mice were sacrificed and tissues harvested, they fasted for 5 h. Mice in the exercise groups had access to their home-cage running wheels until 1–2 h prior to sacrifice. A schematic representation of the study design is provided in Figure 1.

Body composition

Body composition was assessed within the week prior to tissue harvest using a non-invasive nuclear MRI whole-body composition analyzer (EchoMRI 4in1/1100; Echo Medical Systems, Houston, TX). In addition, the adipose tissue distribution was assessed at sacrifice via measurement of visceral (i.e. perigonadal, PGAT), s.c. (inguinal SQAT), and interscapular brown (BAT) adipose tissue. Liver mass was also assessed.

Glucose tolerance, fasting blood biochemistry, and surrogate measures of insulin resistance

Glucose tolerance tests (GTTs) were conducted following a 5-h fast to assess glucose handling. Baseline blood glucose was measured with a hand-held glucometer by pricking the tail with a razor blade. A glucose solution (2 g/kg) was injected intraperitoneally. Blood glucose concentration was then measured via glucometer at 15, 30, 45, 60, and 120 min after the injection. Blood samples were collected during tissue harvest, and the plasma was obtained via centrifugation to assess insulin, glucose, estradiol, and non-esterified fatty acid (NEFA) levels. Insulin and glucose concentrations were obtained via commercially available mouse-specific kits (Crystal Chem, Elk Grove Village, IL; Insulin kit #90080, Glucose kit #81692). Estradiol was assessed using kit #ES180S-100 (CalBioTech, El Cajon, CA). NEFA levels were measured using a kit from ZenBio (Research Triangle Park, NC; Kit: SFA-5). The homeostasis model assessment of insulin resistance (HOMA-IR) is considered a calculated measure of insulin resistance and was calculated using the following equation: fasting insulin in (ng/mL) × glucose in mg/dL/22.5. Adipose tissue insulin resistance (Adipo-IR) was calculated by multiplying the fasting insulin concentration (μU/L) by the fasting NEFA concentration (mmol/L).

Energy expenditure

Energy expenditure (total and resting) and spontaneous physical activity (SPA) were measured via indirect calorimetry using metabolic chambers (Promethion, Sable Systems International, Las Vegas, NV). Expedata software was used to collect data averaged over 12 h light:12 h darkness cycles. Spontaneous physical activity was calculated as the sum of X, Y, and Z beam breaks. Bodyweight and food intake were measured before and after each

assessment. All mice were individually housed in the chambers for 3 days, thus capturing at least two full light and darkness cycles.

Ex vivo adipocyte mitochondrial respiration

Mature adipocyte respiration was assessed using a high-resolution respirometry (Oroboros Oxygraph-2k; Oroboros Instruments, Innsbruck, Austria). Briefly, from a fresh sample of white adipose tissue, floating adipocytes were harvested following separation from the stromal vascular fraction. Isolated mature adipocytes were then loaded into respiration chambers containing buffer MiR05 (100 mM sucrose, 60 mM K-lactobionate, 0.5 mM EGTA, 3 mM MgCl2, 20 mM taurine, 10 mM KH2PO4, 20 mM HEPES, adjusted to pH 7.1 with KOH at 37°C and 1 g/L fatty acid-free BSA) to assess basal respiration. Digitonin (2 μM) was added to the chambers to permeabilize the adipocytes. Glutamate (5 mM) and malate (2 mM) were added to the chambers to assess state 2 respiration in the absence of ADP. State 3, complex I respiration was then assessed by titration of ADP (50–200 μM). The addition of succinate (7.5 mM) allowed for the measurement of state 3, complex I and complex II respiration. Finally, maximal uncoupled respiration was assessed by the addition of carbonyl cyanide 4-(trifluoromethoxy) phenylhydrazone (0.25–0.5 μM).

Adipocyte histology and UCP1 staining

PGAT samples fixed in formalin were submitted to the Veterinary Medical Diagnostic Laboratory (Columbia, MO), where they were processed into 5-μm sections after paraffin embedding and stained for 30 min with UCP1 antibody (1:1200 dilution) using a heat-induced epitope retrieval (HIER) pretreatment, with DAKO citrate in a cloaking chamber. The sections were analyzed using an Olympus BX34 photomicroscope (Olympus), and images were taken using an Olympic SC30 Optical Microscope Accessory CMOS color camera. UCP1 content of 6–10 PGAT cells was quantified for three mice per group using ImageJ software as described previously (Wainright *et al.* 2015). To determine PGAT cell size, three independent regions within the same 40× objective field were selected (50 adipocytes per animal, three animals per group), and the cross-sectional area of each cell was determined via ImageJ software using perimeter tracings.

Gene expression via qRT-PCR

PGAT samples were homogenized in TRIzol solution using a tissue homogenizer (TissueLyser LT, Qiagen). Total RNA was isolated in accordance with the Qiagen's RNeasy lipid tissue protocol, and the concentration and purity were determined using a Nanodrop spectrophotometer (Thermo Scientific). First-strand cDNA was synthesized from total RNA using the High Capacity cDNA RT kit (Applied Biosystems). Quantitative real-time PCR was performed as previously described using the ABI StepOne Plus sequence detection system (Applied Biosystems) (Padilla *et al.* 2013). The NCBI primer Design tool was used to design primer sequences, and all primers were purchased from IDT (Coralville, IA). The housekeeping gene, β actin, cycle threshold (CT) did not differ across groups. The mRNA expression of the analyzed genes was calculated by $2^{\Delta CT}$ where ΔCT = β actin CT – gene of interest CT and was presented as fold-difference. The mRNA levels were normalized to the WTCon group, which was set at 1. A complete list of primer sequences used is provided in Table 1.

Western blot

Protein content was determined as described previously (Winn *et al.* 2017a). In brief, protein samples (10 μg/lane) were separated via SDS-PAGE and transferred to PVDF membranes. They were then probed with primary antibodies. The intensities of the protein bands were quantified using Image Lab Software (Bio-Rad) and expressed as a ratio to total protein stain. A complete list of all antibodies used is provided in Table 2.

Statistics

A 2 × 2 ANOVA was conducted using SPSS V25.0 to assess the effects of genotype (WT vs ERB_{DBD}KO mice) and treatment (control vs wheel running) for all statistical assessments unless otherwise specified. To examine body weight and food intake over time, a multivariate repeated measures ANOVA was conducted, looking at the effects of time, genotype, and treatment. To compare body weight and food intake pre- and post-OVX, paired *t*-tests were performed. All data are presented as the mean ±S.E.M. Results were considered significant at $P \leq 0.05$. Three outliers were removed for analysis of UCP1 protein expression because they exceeded the range of the standard deviation. *P* values for genotype (G), treatment (T), and genotype–treatment interaction (G×T) are listed within the graph space, and values are presented in bold if significant. Asterisks indicate differences between groups if there was a G×T and the *post hoc* test was significant.

Results

Model validation

The ERb_{DBD}KO mouse model was validated via PCR as previously demonstrated (Krege *et al.* 1998) (Fig. 2A). We also validated that the KO groups completely lacked ERbDBD gene expression (G, $P < 0.001$) while expressing similar levels of ERa and full ERb isoform (Fig. 2B). This validates the presence of a mutated ERb protein that lacks exon 3, encoding the DBD (Krege *et al.* 1998), while there were no differences in expression of the full ERb protein (Fig. 2C and D). Successful OVX was confirmed by significant uterine atrophy (mean ± S.E.M. (g): WTCon 0.02 ± 0.00, WTEx 0.03 ± 0.00, KOCon 0.05 ± 0.02, KOEx 0.03 ± 0.01; $P > 0.05$). All groups also exhibited similarly low concentrations of estradiol in plasma, indicating no effect of loss of DBD on circulating estradiol levels (mean ± S.E.M. (pg/mL): WTCon 5.10 ± 0.91, WTEx 4.69 ± 0.79, KOCon 4.10 ± 0.62, KOEx 4.92 ± 0.95; NS).

Effects of OVX on metabolic parameters in WT and KO mice

As expected, OVX increased body weight gain similarly ($P < 0.001$) across groups. Genotype did not affect OVX-induced weight gain or final body weight (Fig. 3A). There were also no differences in food intake (not shown) nor were there differences in voluntary wheel running (Fig. 3B) or exercise-induced increase in energy expenditure (Fig. 3C), allowing us the unique opportunity to assess the independent role of ERbDBD in mediating effects of exercise following OVX. In addition, wheel running access did not affect spontaneous cage physical activity in the active cycle, (Fig. 3D), resting energy expenditure (Fig. 3E), or cage activity in the inactive cycle (Fig. 3F). This is important because it

indicates that they did not 'make up' for the exercise by reducing cage physical activity. There were no differences in the respiratory quotient, indicating no differences in fuel use (data not shown). Energy intake did not differ significantly between genotypes, but Ex mice consumed significantly more energy than Sed mice (T, $P = 0.017$). This effect remained even after adjusting for body weight, highlighting that energy expenditure increases due to exercise were made up for by energy consumption, thus preventing attenuation of weight gain. In summary, exercise did not attenuate OVX-induced weight gain in either genotype due to increased *ad libitum* energy intake.

OVX also predictably caused metabolic dysfunction (i.e. adiposity increase and insulin resistance) similarly in both genotypes. Age-matched littermate ovary-intact WTCon females fed the same HFD had an average of 24.60 ± 1.49% body fat compared to 38.20 ± 2.49% in the OVX WTCon group; KO mice responded similarly to OVX (ovary intact KO: 26.50 ± 3.79% vs OVX KO: 37.40 ± 3.24%). Following OVX, all mice were insulin resistant, as indicated by their blood glucose levels during the glucose tolerance tests as well as the calculated HOMA-IR. Intact WTCon females had an average HOMA-IR of 5.76 ± 1.09 compared with 6.59 ± 1.35 for the OVX WT, and the KO groups responded similarly (ovary-intact KO: 4.55 ± 0.61 vs OVX KO: 6.49 ± 1.39).

From this point forward, comparisons were made between the OVX groups in order to assess the effect of wheel running on OVX-induced metabolic dysfunction in WT compared to KO mice. As shown in Table 3, these groups did not differ significantly with regard to their s.c., perigonadal, and brown adipose tissue pad weights, or liver weights at sacrifice. At sacrifice, there were no significant differences in body weight, relative lean mass or fat mass, or absolute lean mass or fat mass. Although wheel running tended to decrease PGAT cell size in both genotypes (T, $P = 0.06$), the effect was not significant. Thus, overall, exercise did not mitigate OVX-induced weight gain or alter body composition in either genotype.

Effect of genotype and wheel running access on glucose and lipid metabolism

Paradoxically, wheel running significantly increased fasting plasma insulin levels (T, $P < 0.05$), an effect largely driven by the KO group, which trended toward having greater insulin levels compared to WT (G, $P = 0.09$) (Table 4). There were also significant treatment (T, $P < 0.05$) and genotype effects (G, $P < 0.05$), as well as a genotype × treatment interaction (G×T, $P < 0.05$) for HOMA-IR, an indicator of insulin resistance, which was also driven by the high values in the KOEx group (i.e. exercise increased insulin resistance in the KO but not WT group) (Fig. 4A). Similarly, there was a significant treatment (T, $P < 0.05$) and genotype effect (G, $P < 0.05$) for Adipo-IR, an indicator of adipose tissue insulin resistance, which, again, was driven by the KO group responding adversely to exercise (Fig. 4B).

The KO groups tended to exhibit higher NEFA levels than the WT groups (G, $P = 0.06$), whereas no other differences were significant or approached significance (Table 4). Overall, the results suggest that exercise adversely affected systemic metabolism in KO mice.

Effect of genotype and wheel running on WAT immunometabolism

The KO groups exhibited a lower relative gene expression of adiponectin (G, $P < 0.05$) (Fig. 4C). However, there was no significant difference in the leptin:adiponectin ratio, which is

generally considered to reflect the inflammatory tone of the adipose tissue. Interestingly, WT and KO groups responded differently to exercise with regard to TNFa expression such that exercise unexpectedly increased the expression of TNFa in the KO mice only (G×T, $P < 0.01$) (Fig. 4C). After finding this evidence of WAT inflammation, we next measured inflammatory proteins in WAT. As shown in Fig. 5, unlike gene expression differences, the increase in TNFa protein expression did not reach statistical significance. There were also no effects of genotype or wheel running on NFkB (an inflammatory transcription factor) or MCP1 (an inflammatory chemokine). However, wheel running exercise significantly reduced WAT adiponectin levels, implicating exercise as having an inflammatory effect in the setting of OVX.

Effect of genotype and wheel running access on browning of WAT

Exercise-induced adipocyte browning was clearly visible in the WT mice, as indicated by increased multilocular phenotype (Fig. 6A), suggesting for the first time that OVX female mice are capable of experiencing exercise-induced adipose tissue browning. There was a higher density of WAT UCP1 staining upon wheel running exercise in the WT mice (Fig. 6B) which was also validated by WAT UCP1 protein quantification (Fig. 6C and D). Remarkably, this effect was completely absent in the KO mice, who also had a significantly lower WAT gene expression of UCP1 (Fig. 6E).

Effect of genotype and wheel running access on adipocyte mitochondrial metabolism

Although exercise increased WAT UCP1 content, this did not associate with increased mitochondrial content. That is, there were no significant genotype or treatment effects with regard to the oxidative phosphorylation (OXPHOS) complexes I–V in WAT (Fig. 7A and B), nor were there differences in OX PHOS gene expression, with the exception of COX4, which was significantly higher in the KO groups (G, $P < 0.05$) (Fig. 7C). We next isolated adipocytes from WAT and assessed O_2 consumption as an indictor of mitochondrial activity. Similar to the divergent exercise-induced UCP1 responses, there was a G×T ($P = 0.02$) in adipocyte basal mitochondrial O_2 consumption, such that adipocytes harvested from the WTEx mice, but not KOEx group, increased relative to their respective controls (Fig. 7D). However, no measures of substrate-stimulated mitochondrial respiration were significantly impacted by genotype or treatment. Attempts to assess WAT adipocyte mitochondrial morphological differences between genotypes with and without exercise training via TEM were not successful due to the low copy number of mitochondria in white adipocytes. In order to at least crudely assess mitochondrial morphology differences, we performed TEM on brown adipocytes, since mitochondria are plentiful in brown adipose tissue. Here, we did not find significant differences (data not shown).

Discussion

Loss of ovarian hormones in humans and rodents leads to adipose tissue-specific metabolic dysfunction, a critical predictor of the metabolic diseases that follow menopause. We demonstrated in a series of studies that both the absence of uncoupling protein 1 (UCP1) (Clookey *et al.* 2018) and absence of estrogen receptor beta (ERb) exacerbate ovariectomy (OVX)-induced metabolic dysfunction, whereas the absence of ERa does not affect OVX

responses (Zidon *et al.* 2020). We have also shown that the pharmacological activation of UCP1 completely rescues metabolic dysfunction (Clookey *et al.* 2019). The present study was the first to investigate the role of ERb's classical genomic actions in mediating adipose tissue-specific responses to exercise. The major findings were: (1) lack of ERbDBD did not affect OVX-associated weight gain, food intake, or voluntary wheel running, allowing for the investigation of ERbDBD-mediated responses to wheel running exercise independent of those potential confounds. Both genotypes responded as expected following OVX, a phenotype well characterized by our group and others (Hong *et al.* 2009). (2) Despite no genotype differences in response to exercise in terms of body composition or energy intake/utilization, genotype differences were observed in adipocyte-specific mitochondrial adaptations to exercise. Among the most striking and novel observations were that the ERbDBD was required for exercise-induced beigeing, and its absence coincided with increased adipose tissue (i.e. Adipo-IR) and systemic (i.e. HOMA-IR) insulin resistance.

Beigeing of white adipose tissue is metabolically beneficial, contributing to increased insulin sensitivity (Clookey *et al.* 2018). Thus, exercise-mediated browning, which has been demonstrated in some (Aldiss *et al.* 2019) but not all previous studies (Ponnusamy *et al.* 2017, Otero-Díaz *et al.* 2018, Aldiss *et al.* 2019), may help explain at least some of the beneficial effects of exercise on insulin sensitivity. Numerous studies have shown housing temperature below thermoneutrality is required for exercise-induced beigeing (McKie *et al.* 2019, Raun *et al.* 2020, Aldiss *et al.* 2020). Thus, it would not be expected that the mice in the current study (housed at thermoneutrality) would exhibit beigeing, and thus, it is interesting that the WT mice in this study did show signs of beigeing, despite not being cold stressed. This discrepancy might be due to the fact that the mice in the present study had undergone OVX. To our knowledge, no prior studies have assessed exercise-induced browning following OVX. It may be that OVX makes rodents less 'stress tolerant' and thus, the stress of exercise even at thermoneutrality is sufficient to induce browning. The hypothesis that OVX affects sensitivity to exercise-mediated beigeing should be tested in future studies. Indeed, a limitation of the current study is that the ovary-intact control WT and KO mice were not assessed for exercise responses. Because the purpose of this study was to examine the effects of genotype and exercise in the setting of OVX, the assessment of ovary-intact mice was outside the scope. Future studies should assess the role of ERbDBD on exercise-mediated beigeing in the ovary-intact state.

It is noteworthy that the effects of the exercise demonstrated in this current study were independent of fat loss. Thus, the modest induction of UCP1 in the WT mice was not sufficient to increase energy expenditure enough to induce weight loss. The fact that UCP1 induction was completely absent in ERb_{DBD}KO mice implicates ERbDBD as playing an integral role in exercise-mediated WAT browning in the setting of OVX. Especially in light of recent evidence that UCP1 expression is required for optimal insulin sensitivity (Winn *et al.* 2017*a*,b) in both sexes, including in the setting of OVX (Clookey *et al.* 2018), this finding may have critical implications regarding the efficacy of exercise to improve adipocyte health following hormone loss. Although exercise was not sufficient to improve systemic indicators of insulin sensitivity in either genotype, it is interesting and notable that the absence of an exercise-mediated increase in WAT UCP1 coincided with an unexpected *increase* in surrogate markers of insulin resistance following exercise training in the KO mice. This

finding aligns with our previous work that showed that UCP1KO mice are more adversely affected by OVX, suggesting that UCP1 is protective following OVX. We reason that (1) voluntary wheel running is not sufficient to mitigate the insulin resistance caused by the combination of OVX + high-fat diet and (2) without a compensatory increase in UCP1; exercise stress may actually increase insulin resistance. It is important to note that we did not directly assess tissue-specific or systemic insulin sensitivity in this study, and thus, our data represent indirect measures of insulin sensitivity. Future studies should perform glucose clamps to more directly assess insulin sensitivity.

The mechanisms involved in exercise-induced adipocyte browning are not well understood. It may be that increased NEFAs during exercise may stimulate UCP1 activity (Virtanen *et al.* 2014), but specific factors responsible for UCP1 transcription and translation remain elusive. UCP1 is a nuclear-encoded protein (Ledesma *et al.* 2002). Since ERa and ERb both act as ligand-activated nuclear transcription factors, UCP1 may be induced by ERa and/or ERb. Notably, females, who have greater levels of circulating estrogen, also have greater levels of UCP1 expression. Moreover, there is now evidence that ERa is necessary for adipocyte mitochondrial remodeling and UCP1-mediated uncoupled respiration (Zhou *et al.* 2020). Here, we used ERb_{DBD}KO mice to test whether ERb genomic activity is required for UCP1 induction. The lack of UCP1 protein upregulation in the KO may support that UCP1 is regulated in some way by ERb. Since UCP1 mRNA was not affected, this suggests that the role played by ERbDBD is indirect. Interestingly, our previous work indicated that exercise robustly induces ERb protein expression in WAT, which correlates strongly with UCP1 in rodents and humans (Porter *et al.* 2020). The data presented herein support our working hypothesis, that, like ERa, ERb plays a critical role in adipocyte mitochondrial metabolism. Exercise-mediated ERb upregulation may enable exercise-induced UCP1. Further work is necessary to determine the mechanism by which exercise induces ERb expression and whether estrogen/ERb binding directly or indirectly affects UCP1.

It is unclear why it would be advantageous for exercise to induce browning. It has been suggested that UCP1 buffers mitochondrial ROS (Oelkrug *et al.* 2014) and thus may protect against ROS-induced inflammation associated with the mitochondrial activity. This may lend insight into why the KO mice experienced an atypical increase in adipose tissue TNFa gene expression with exercise, coinciding with their absence of UCP1 response. It may be that an exercise-mediated increase in the mitochondrial activity must be coupled with an appropriate increase in UCP1 in order to buffer the increased ROS and inflammation associated with exercise. In other words, without an adequate upregulation of UCP1, exercise may increase adipose tissue inflammation and *increase* insulin resistance. Indeed, evidence from our group and others clearly demonstrates that UCP1 is a critical insulin-sensitizing protein (Winn *et al.* 2017a). The present findings may suggest that an exercise-mediated increase in UCP1 is necessary for exercise-mediated improvements in insulin sensitivity (Fig. 8). Since ERb is expressed on many cell types, including immune cells (Paterni *et al.* 2014), the inflammatory response in the KO may also have been attributed to direct effects on immune cells. Indeed, targeting macrophage ERb has been shown to have anti-inflammatory effects (Wang *et al.* 2019).

ERb is known to localize in mitochondria, and studies have shown that exercise positively influences mitochondrial outcomes in adipose tissue (Mendham *et al.* 2020). We did not observe robust differences in mitochondrial activity, but we did observe an upregulation of COX4 gene expression in the KO mice. The COX4 gene is the largest nucleus-encoded subunit of cytochrome c oxidase, the terminal enzyme complex of the mitochondrial electron transport chain. In addition to the DBD lacking, the possibility exists that the mutant mice may display an upregulation in the non-genomic functions of ERb. One such function may be associated with ERb's mitochondrial sequestration. Based on the evidence that ERb affects adipocyte mitochondria (Wollheim 2000, Ponnusamy *et al.* 2017), we hypothesized that the KO mice would be less responsive to the beneficial effects of exercise on adipocyte mitochondria. Supporting this, we found that basal adipocyte mitochondrial respiration was differentially affected by exercise such that it increased in the WT but decreased in the KO (Fig. 7).

No previous studies have investigated how lack of ERb genomic function affects exercise-mediated metabolic adaptations. ERb has actually been shown in previous studies to contribute to insulin resistance, possibly via the suppression of skeletal muscle GLUT4 expression (Barros *et al.* 2009). However, we found no differences in GLUT4 gene or protein expression. Another possibility is that the exacerbated insulin resistance may be related to the regulatory action of ERb observed by Soriano *et al.* (2009) on the K_{ATP} channels of the pancreatic beta cells. In pancreatic beta cells, mitochondrial ATP generation in response to glucose oxidation is required for the secretion of insulin. Thus, increased ATP production in the KOEx mice may have increased insulin secretion, resulting in the hyperinsulinemia observed. This should be tested in future studies.

Similar to menopause in humans, OVX causes obesity and insulin resistance in rodents (Stachowiak *et al.* 2015). The fact that the voluntary exercise intervention did not positively impact metabolic dysfunction supports the idea that postmenopausal women may require a net energy deficit achieved possibly via more vigorous exercise or longer exercise intervention.

The findings of the present study should be considered in light of its limitations. First, OVX is a widespread and well-established rodent model of human menopause (Diaz Brinton 2012), but while this surgery causes a sharp decline in E_2 production, menopause often occurs gradually and is associated with a critical perimenopause period (Santoro 2016). Secondly, the mutant model here is not a complete ERbKO; thus, the findings cannot be extrapolated to indicate the effects of eliminating all of ERb functions. Thirdly, only surrogate measures of insulin sensitivity were used. Finally, despite prior studies showing exercise-induced browning of SQAT, only visceral fat was assessed here – the decision to focus only on PGAT and not SQAT was due to the fact that, unlike browning of SQAT where males and females appear equally sensitive, there are known sex differences in browning of PGAT (Kim 2016). We focused our attention and available resources on PGAT in particular to assess the potential role of ERb in that sex difference, but future studies should determine the role of ERb in exercise-induced browning of SQAT.

In conclusion, we validate that exercise-induced WAT browning occurs following OVX in female mice and further show that ERbDBD is necessary for this effect. Not only were the mutant mice completely resistant to WAT browning but they responded adversely to exercise, as indicated by increased insulin resistance and a subtle yet significant increase in TNFa gene expression. In the future, creating adipocyte-specific ERbKO mice could aid in uncovering the mechanism by which ERb mediates exercise-induced browning. Increasing our knowledge of the metabolic effects of ERb signaling will have broad applications, including the development of ERb-agonist drugs that provide metabolic protection to not only postmenopausal women but also other metabolically dysfunctional populations.

Acknowledgements

The authors thank DeAna Grant of the University of Missouri Electron Microscopy Core Facility for processing and imaging the adipose tissue mitochondria, as well as to Elyse Frazier and Candace Rowles for their assistance with histological analyses.

Funding

Funded by internal research grants from the University of Missouri to V J Vieira-Potter. This work was supported in part by a VA-Merit Grant I01BX003271 (R S Rector), and NIH R01 HL094404 (C P Baines). This work was supported with resources and the use of facilities at the Harry S. Truman Memorial Veterans Hospital in Columbia, MO.

References

Aldiss P, Lewis JE, Lupini I, Boocock DJ, Miles AK, Ebling FJP, Budge H & Symonds ME 2019 Exercise does not induce browning of WAT at thermoneutrality and induces an oxidative, myogenic signature in BAT. bioRxiv 649061. (10.1101/649061)

Aldiss P, Lewis JE, Lupini I, Bloor I, Chavoshinejad R, Boocock DJ, Miles AK, Ebling FJP, Budge H & Symonds ME 2020 Exercise training in obese rats does not induce browning at thermoneutrality and induces a muscle-like signature in brown adipose tissue. Frontiers in Endocrinology 11 97. (10.3389/fendo.2020.00097) [PubMed: 32265830]

Barros RPA, Gabbi C, Morani A, Warner M & Gustafsson JA 2009 Participation of ERα and ERβ in glucose homeostasis in skeletal muscle and white adipose tissue. American Journal of Physiology: Endocrinology and Metabolism 297 E124–E133. (10.1152/ajpendo.00189.2009) [PubMed: 19366879]

Clookey SL, Welly RJ, Zidon TM, Gastecki ML, Woodford ML, Grunewald ZI, Winn NC, Eaton D, Karasseva NG, Sacks HS, et al. 2018 Increased susceptibility to OVX-associated metabolic dysfunction in UCP1-null mice. Journal of Endocrinology 239 107–120. (10.1530/JOE-18-0139)

Clookey SL, Welly RJ, Shay D, Woodford ML, Fritsche KL, Rector RS, Padilla J, Lubahn DB & Vieira-Potter VJ 2019 Beta 3 adrenergic receptor activation rescues metabolic dysfunction in female estrogen receptor alpha-null mice. Frontiers in Physiology 10 9. (10.3389/fphys.2019.00009) [PubMed: 30804793]

Deroo BJ & Korach KS 2006 Estrogen receptors and human disease. Journal of Clinical Investigation 116 561–570. (10.1172/JCI27987)

Diaz Brinton R 2012 Minireview: translational animal models of human menopause: challenges and emerging opportunities. Endocrinology 153 3571–3578. (10.1210/en.2012-1340) [PubMed: 22778227]

Giralt M & Villarroya F 2013 White, brown, beige/brite: different adipose cells for different functions? Endocrinology 154 2992–3000. (10.1210/en.2013-1403) [PubMed: 23782940]

Hong J, Stubbins RE, Smith RR, Harvey AE & Núñez NP 2009 Differential susceptibility to obesity between male, female and ovariectomized female mice. Nutrition Journal 8 11. (10.1186/1475-2891-8-11) [PubMed: 19220919]

Kautzky-Willer A, Harreiter J & Pacini G 2016 Sex and gender differences in risk, pathophysiology and complications of type 2 diabetes mellitus. Endocrine Reviews 37 278–316. (10.1210/er.2015-1137) [PubMed: 27159875]

Kim SN, Jung YS, Kwon HJ, Seong JK, Granneman JG & Lee YH 2016 Sex differences in sympathetic innervation and browning of white adipose tissue of mice. Biology of Sex Differences 7 67. (10.1186/s13293-016-0121-7) [PubMed: 27990249]

Klinge CM 2008 Estrogenic control of mitochondrial function and biogenesis. Journal of Cellular Biochemistry 105 1342–1351. (10.1002/jcb.21936) [PubMed: 18846505]

Kozakowski J, Gietka-Czernel M, Leszczyńska D & Majos A 2017 Obesity in menopause – our negligence or an unfortunate inevitability? Menopause Review 16 61–65. (10.5114/pm.2017.68594) [PubMed: 28721132]

Krege JH, Hodgin JB, Couse JF, Enmark E, Warner M, Mahler JF, Sar M, Korach KS, Gustafsson JA & Smithies O 1998 Generation and reproductive phenotypes of mice lacking estrogen receptor β. PNAS 95 15677–15682. (10.1073/pnas.95.26.15677) [PubMed: 9861029]

Kusminski CM & Scherer PE 2012 Mitochondrial dysfunction in white adipose tissue. Trends in Endocrinology and Metabolism 23 435–443. (10.1016/j.tem.2012.06.004) [PubMed: 22784416]

Ledesma A, de Lacoba MG & Rial E 2002 The mitochondrial uncoupling proteins. Genome Biology 3 reviews3015.1–reviews3015.9. (10.1186/gb-2002-3-12-reviews3015) [PubMed: 12537581]

Liao TL, Tzeng CR, Yu CL, Wang YP & Kao SH 2015 Estrogen receptor-β in mitochondria: implications for mitochondrial bioenergetics and tumorigenesis. Annals of the New York Academy of Sciences 1350 52–60. (10.1111/nyas.12872) [PubMed: 26301952]

Madak-Erdogan Z, Kieser KJ, Kim SH, Komm BN, Katzenellenbogen JA & Katzenellenbogen BS 2008 Nuclear and extranuclear pathway inputs in the regulation of global gene expression by estrogen receptors. Molecular Endocrinology 22 2116–2127. (10.1210/me.2008-0059) [PubMed: 18617595]

McKie GL, Medak KD, Knuth CM, Shamshoum H, Townsend LK, Peppler WT & Wright DC 2019 Housing temperature affects the acute and chronic metabolic adaptations to exercise in mice. Journal of Physiology 597 4581–4600. (10.1113/JP278221)

Mendham AE, Larsen S, George C, Adams K, Hauksson J, Olsson T, Fortuin-de Smidt MC, Nono Nankam PA, Hakim O, Goff LM, et al. 2020 Exercise training results in depot-specific adaptations to adipose tissue mitochondrial function. Scientific Reports 10 3785. (10.1038/s41598-020-60286-x) [PubMed: 32123205]

Oelkrug R, Goetze N, Meyer CW & Jastroch M 2014 Antioxidant properties of UCP1 are evolutionarily conserved in mammals and buffer mitochondrial reactive oxygen species. Free Radical Biology and Medicine 77 210–216. (10.1016/j.freeradbiomed.2014.09.004) [PubMed: 25224037]

Otero-Díaz B, Rodríguez-Flores M, Sánchez-Muñoz V, Monraz-Preciado F, Ordoñez-Ortega S, Becerril-Elias V, Baay-Guzmán G, Obando-Monge R, Garcia-Garcia E, Palacios-González B, et al. 2018 Exercise induces white adipose tissue browning Across the weight spectrum in humans. Frontiers in Physiology 9 1781. (10.3389/fphys.2018.01781) [PubMed: 30618796]

Padilla J, Jenkins NT, Roberts MD, Arce-Esquivel AA, Martin JS, Laughlin MH & Booth FW 2013 Differential changes in vascular MRNA levels between rat iliac and renal arteries produced by cessation of voluntary running. Experimental Physiology 98 337–347. (10.1113/expphysiol.2012.066076) [PubMed: 22709650]

Paterni I, Granchi C, Katzenellenbogen JA & Minutolo F 2014 Estrogen receptors alpha (ERα) and beta (ERβ): subtype-selective ligands and clinical potential. Steroids 90 13–29. (10.1016/j.steroids.2014.06.012) [PubMed: 24971815]

Ponnusamy S, Tran QT, Harvey I, Smallwood HS, Thiyagarajan T, Banerjee S, Johnson DL, Dalton JT, Sullivan RD, Miller DD, et al. 2017 Pharmacologic activation of estrogen receptor β increases mitochondrial function, energy expenditure, and Brown adipose tissue. FASEB Journal 31 266–281. (10.1096/fj.201600787RR) [PubMed: 27733447]

Porter JW, Barnas JL, Welly R, Spencer N, Pitt J, Vieira-Potter VJ & Kanaley JA 2020 Age, sex, and depot-specific differences in adipose-tissue estrogen receptors in individuals with obesity. Obesity 28 1698–1707. (10.1002/oby.22888) [PubMed: 32734695]

Raun SH, Henriquez-Olguín C, Karavaeva I, Ali M, Møller LLV, Kot W, Castro-Mejía JL, Nielsen DS, Gerhart-Hines Z, Richter EA, et al. 2020 Housing temperature influences exercise training adaptations in mice. Nature Communications 11 1560. (10.1038/s41467-020-15311-y)

Santoro N 2016 Perimenopause: From research to practice. Journal of Women's Health 25 332–339. (10.1089/jwh.2015.5556)

Soriano S, Ropero AB, Alonso-Magdalena P, Ripoll C, Quesada I, Gassner B, Kuhn M, Gustafsson JA & Nadal A 2009 Rapid Regulation of KATP Channel Activity by 17β-estradiol in Pancreatic β-Cells Involves the estrogen receptor β and the atrial natriuretic peptide Receptor. Molecular Endocrinology 23 1973–1982. (10.1210/me.2009-0287) [PubMed: 19855088]

Stachowiak G, Pertyński T & Pertyńska-Marczewska M 2015 Metabolic disorders in menopause. Menopause Review 14 59–64. (10.5114/pm.2015.50000) [PubMed: 26327890]

Stallknecht B, Vinten J, Ploug T & Galbo H 1991 Increased activities of mitochondrial enzymes in white adipose tissue in trained rats. American Journal of Physiology 261 E410–E414. (10.1152/ajpendo.1991.261.3.E410)

Stanford KI, Middelbeek RJW & Goodyear LJ 2015 Exercise effects on white adipose tissue: beiging and metabolic adaptations. Diabetes 64 2361–2368. (10.2337/db15-0227) [PubMed: 26050668]

Virtanen KA 2014 BAT thermogenesis: linking shivering to exercise. Cell Metabolism 19 352–354. (10.1016/j.cmet.2014.02.013) [PubMed: 24606895]

Wainright KS, Fleming NJ, Rowles JL, Welly RJ, Zidon TM, Park YM, Gaines TL, Scroggins RJ, Anderson-Baucum EK, Hasty AH, et al. 2015 Retention of sedentary obese visceral white adipose tissue phenotype with intermittent physical activity despite reduced adiposity. American Journal of Physiology: Regulatory, Integrative and Comparative Physiology 309 R594–R602. (10.1152/ajpregu.00042.2015)

Wake R & Yoshiyama M 2009 Gender differences in ischemic heart disease. Recent Patents on Cardiovascular Drug Discovery 4 234–240. (10.2174/157489009789152249) [PubMed: 19545234]

Wang L, Zhao RP, Song XY & Wu WF 2019 Targeting ERβ in macrophage reduces crown-like structures in adipose tissue by inhibiting osteopontin and HIF-1α. Scientific Reports 9 15762. (10.1038/s41598-019-52265-8) [PubMed: 31673032]

Winn NC, Vieira-Potter VJ, Gastecki ML, Welly RJ, Scroggins RJ, Zidon TM, Gaines TL, Woodford ML, Karasseva NG, Kanaley JA, et al. 2017a Loss of UCP1 exacerbates western diet-induced glycemic dysregulation independent of changes in body weight in female mice. American Journal of Physiology: Regulatory, Integrative and Comparative Physiology 312 R74–R84. (10.1152/ajpregu.00425.2016)

Winn NC, Grunewald ZI, Gastecki ML, Woodford ML, Welly RJ, Clookey SL, Ball JR, Gaines TL, Karasseva NG, Kanaley JA, et al. 2017b Deletion of UCP1 enhances ex vivo aortic vasomotor function in female but not male mice despite similar susceptibility to metabolic dysfunction. American Journal of Physiology: Endocrinology and Metabolism 313 E402–E412. (10.1152/ajpendo.00096.2017) [PubMed: 28655717]

Winn NC, Jurrissen TJ, Grunewald ZI, Cunningham RP, Woodford ML, Kanaley JA, Lubahn DB, Manrique-Acevedo C, Rector RS, Vieira-Potter VJ, et al. 2019 Estrogen receptor-α signaling maintains immunometabolic function in males and is obligatory for exercise-induced amelioration of nonalcoholic fatty liver. American Journal of Physiology: Endocrinology and Metabolism 316 E156–E167. (10.1152/ajpendo.00259.2018) [PubMed: 30512987]

Wollheim CB 2000 Beta-cell mitochondria in the regulation of insulin secretion: a new culprit in Type II diabetes. Diabetologia 43 265–277. (10.1007/s001250050044) [PubMed: 10768087]

Yepuru M, Eswaraka J, Kearbey JD, Barrett CM, Raghow S, Veverka KA, Miller DD, Dalton JT & Narayanan R 2010 Estrogen receptor-{beta}-selective ligands alleviate high-fat diet- and ovariectomy-induced obesity in mice. Journal of Biological Chemistry 285 31292–31303. (10.1074/jbc.M110.147850)

Zhou Z, Moore TM, Drew BG, Ribas V, Wanagat J, Civelek M, Segawa M, Wolf DM, Norheim F, Seldin MM, et al. 2020 Estrogen receptor α controls metabolism in white and brown adipocytes by regulating Polg1 and mitochondrial remodeling. Science Translational Medicine 12 aax8096. (10.1126/scitranslmed.aax8096)

Zidon TM, Padilla J, Fritsche KL, Welly RJ, McCabe LT, Stricklin OE, Frank A, Park Y, Clegg DJ, Lubahn DB, et al. 2020 Effects of ERβ and ERα on OVX-induced changes in adiposity and insulin resistance. Journal of Endocrinology 245 165–178. (10.1530/JOE-19-0321)

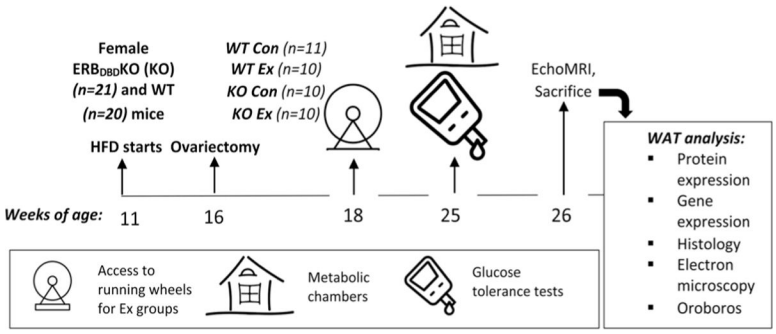

Figure 1.

Study design. Female ERB$_{DBD}$KO (KO) (**n** = 20) and littermate WT control mice (**n** = 21) were individually housed under thermoneutral conditions (26–28°C) and a 12 h light:12 h darkness cycle. Beginning at ~11 (range 10.5–11.5) weeks of age, mice were provided a high-fat diet (46.4% fat: 36.0% carbohydrate: 17.6% protein) **ad libitum** prior to being ovariectomized at 16 weeks of age. Following a 2-week recovery period, mice in the exercise ('Ex') group were provided running wheels whereas control ('Con') mice were not provided wheels. One week prior to sacrifice, total and resting energy expenditure and spontaneous physical activity were assessed in metabolic chambers, and glucose tolerance was determined via glucose tolerance testing. Body composition was measured via EchoMRI, and after sacrifice, white adipose tissue (WAT) was harvested and analyzed as described. HFD, high-fat diet.

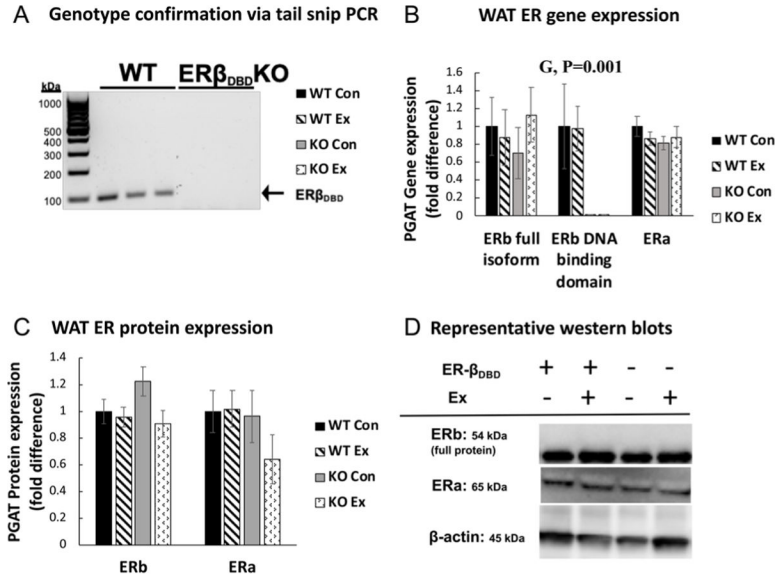

Figure 2.

Genotype validation and white adipose tissue estrogen receptor gene and protein expression. (A) Representative PCR indicating genotype validation. (B) Relative mRNA expression of estrogen receptor beta and estrogen receptor alpha (ERa) in perigonadal white adipose tissue (PGAT). Gene expression was normalized to the housekeeping gene, beta actin and expressed relative to WT control (Con) group. (C) Protein expression of ERb and ERa. (C) Representative western blot bands of ERb, ERa, and housekeeping protein beta actin. Error bars indicate S.E.M. **P** ≤ 0.05 was considered significant; non-significant **P** values not indicated. N_{WTCon} = 11, N_{WTEx} = 10, N_{KOCon} = 10, N_{KOEx} = 10. G, genotype effect; T, treatment effect; G×T, genotype × treatment interaction effect.

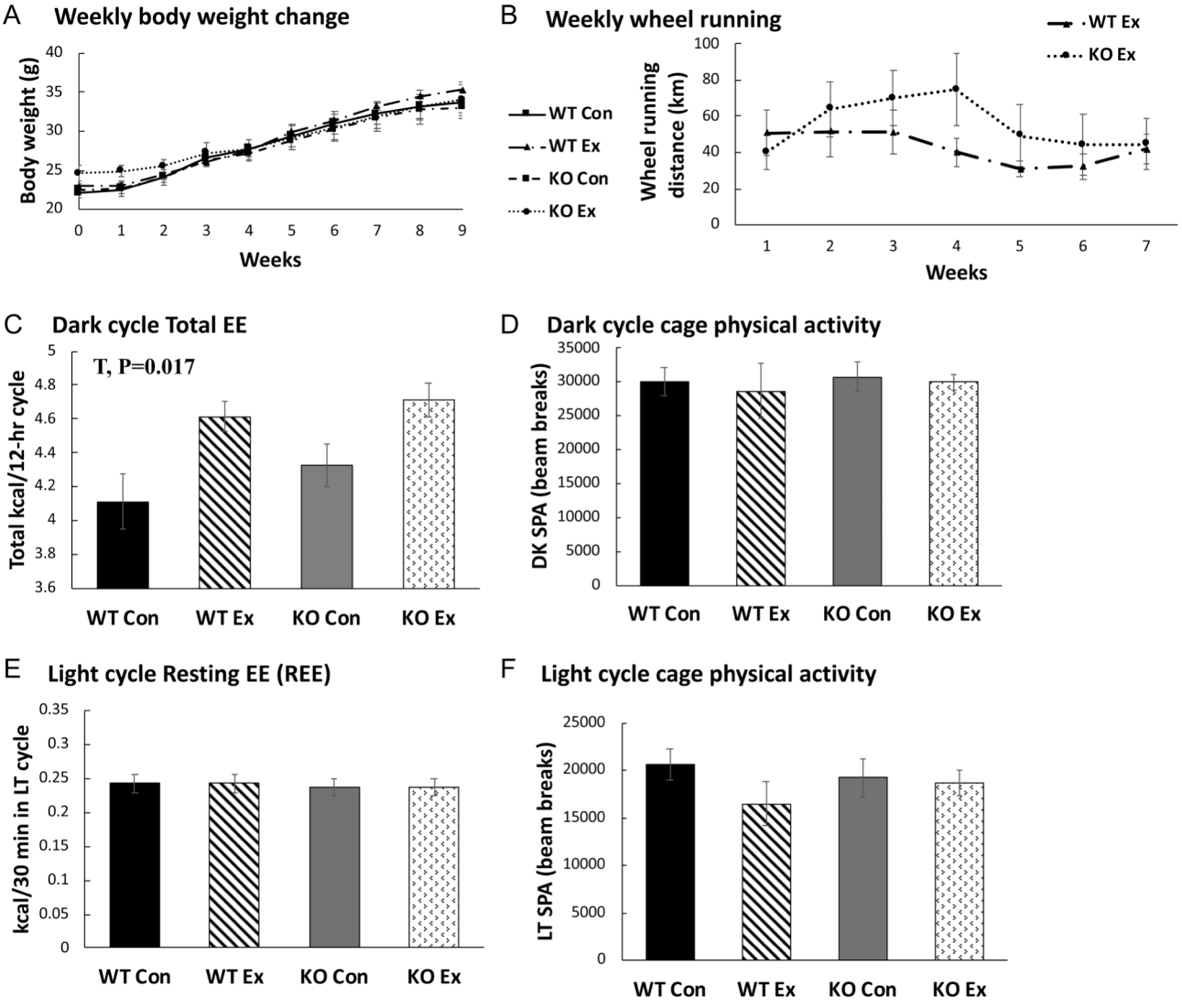

Figure 3.

Measures of energy balance. (A) Body weight throughout study period. (B) Weekly wheel running distance. (C) Total energy expenditure (EE) in darkness cycle (DK) covaried for lean mass. (D) Darkness cycle spontaneous physical activity (SPA). (E) Light cycle resting EE (measured in LT cycle and covaried for lean mass). (F) Light cycle SPA. N_{WTCon} = 8–11, N_{WTEx} = 8–10, N_{KOCon} = 8–10, N_{KOEx} = 9–10. For all graphs, error bars indicate S.E.M. **P** ≤ 0.05 was considered significant; non-significant **P** values are not indicated. G, genotype effect; T, treatment effect; G×T, = genotype × treatment interaction effect.

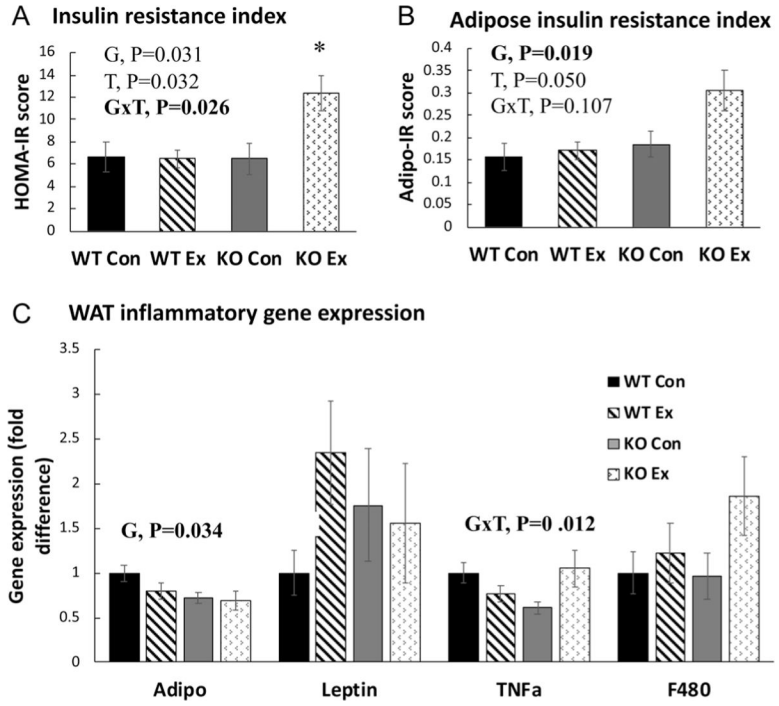

Figure 4.

Insulin resistance (IR) and adipose tissue inflammatory gene expression. (A) HOMA-IR, calculated as the product of fasting blood glucose and plasma insulin levels. (B) Adipo-IR, calculated as the product of non-esterified fatty acid levels and plasma insulin levels. (C) Perigonadal white adipose tissue (PGAT) inflammatory gene expression. Adipo, adiponectin; TNFa, tumor necrosis factor alpha. Gene expression was normalized to the housekeeping gene beta-actin and then expressed relative to WT Con group. Error bars indicate S.E.M. **P** ≤ 0.05 was considered significant; non-significant **P** values were not shown. *KO Ex group was significantly different from the other groups. N_{WTCon} = 11, N_{WTEx} = 10, N_{KOCon} = 10, N_{KOEx} = 10. G, genotype effect; T, treatment effect; G×T, genotype × treatment interaction effect.

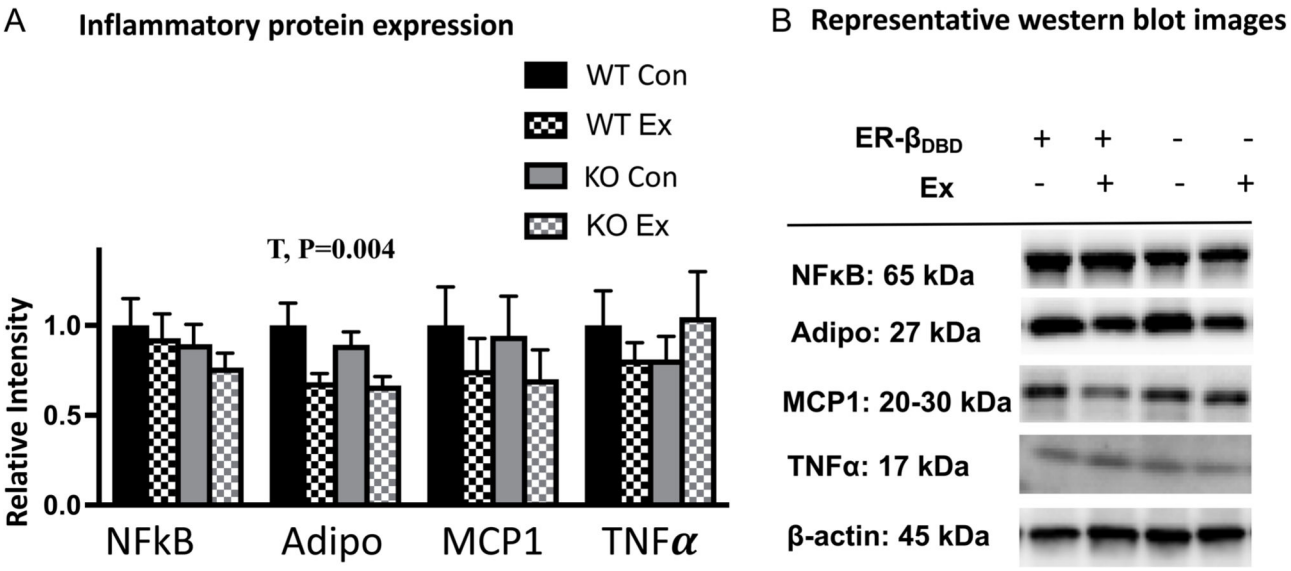

Figure 5.

Adipose tissue inflammatory protein expression. (A) Protein expression of inflammatory proteins via Western blot. (B) Representative bands. Error bars indicate S.E.M. **P** ≤ 0.05 was considered significant; non-significant **P** values were not indicated. NWTCon = 11, NWTEx = 10, NKOCon = 10, NKOEx = 10. G, genotype effect; T, treatment effect.

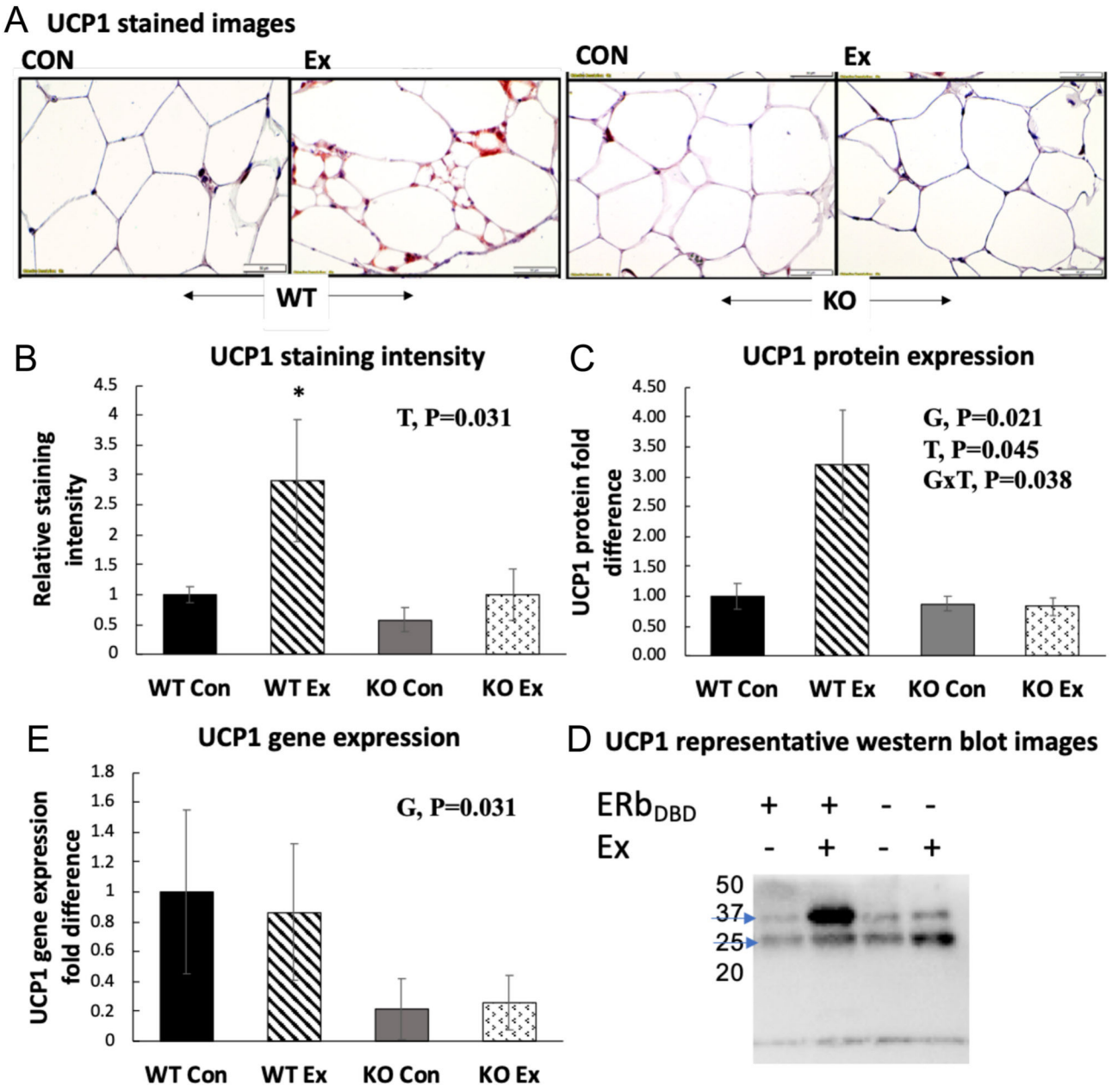

Figure 6.

White adipose tissue browning. (A) Representative images of UCP1 histological staining in perigonadal white adipose tissue (PGAT). (B) Relative PGAT UCP1 staining intensity normalized to WTCon group (**n** = 4–5/group). (C) PGAT UCP1 protein expression and representative Western blot images. (D) PGAT UCP1 gene expression. (E) Mitochondrial OX PHOS protein expression and representative Western blot images. Gene and protein expression data were normalized to the housekeeping gene/protein, beta-actin and expressed relative to WTCon group. Error bars indicate S.E.M. **P** ≤ 0.05 was considered significant; non-significant **P** values were not shown. *WT Ex group was significantly different from all other groups via **post hoc** Tukey's test. G, genotype effect; T, treatment effect; G×T, genotype × treatment interaction effect. Arrows indicate bands of interest.

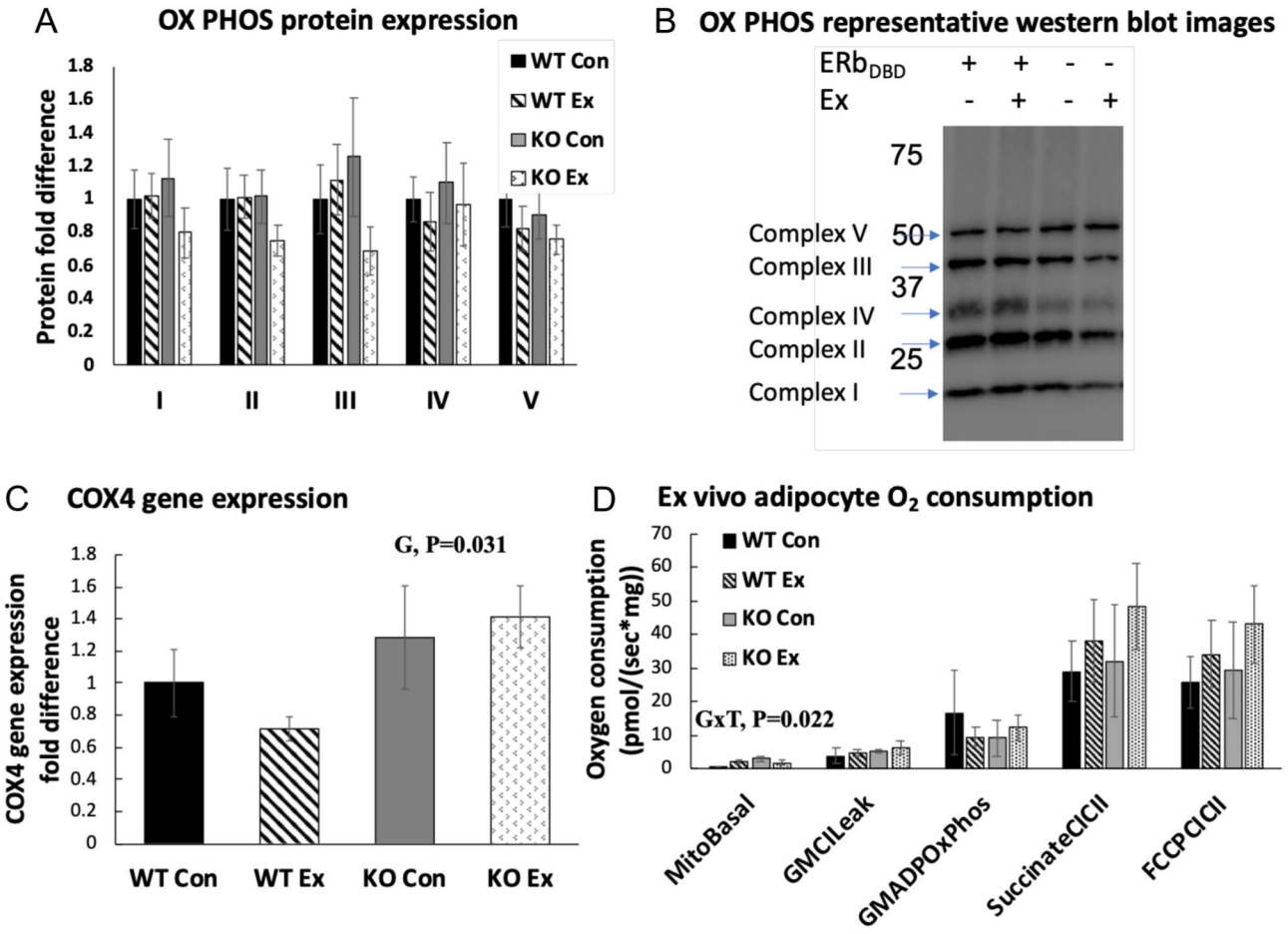

Figure 7.

Measures of white adipocyte browning and mitochondrial activity. (A) WAT mitochondrial OX PHOS protein expression. (B) Representative Western blot images. (C) PGAT COX4 (mitochondrial content indicator) gene expression. (D) PGAT O2 consumption normalized to WT Con group. MitoBasal: 100 mM sucrose, 60 mM K-lactobionate, 0.5 mM EGTA, 3 mM MgCl2, 20 mM taurine, 10 mM KH2PO4, 20 mM HEPES, adjusted to pH 7.1 with KOH at 37°C and 1 g/L fatty acid-free BSA, assessment of basal respiration. GMCILeak: glutamate (5 mM) and malate (2 mM) added, assessment of respiration in absence of ADP. GMADPOxPhos: titration of ADP (50–200 uM), assessment of complex I respiration. SuccinateCICII: addition of succinate (7.5 mM), assessment of state 3, complex I and complex II respiration. FCCPCICII: addition of carbonyl cyanide 4-(trifluoromethoxy) phenylhydrazone (0.25–0.5 uM), assessment of maximal uncoupled respiration (**n** = 3–4/group). Gene and protein expression data were normalized to the housekeeping gene/protein, beta-actin and expressed relative to WT Con group. Error bars indicate S.E.M. **P** ≤ 0.05 was considered significant; non-significant P values were not shown. G, genotype effect; T, treatment effect; G×T, genotype × treatment interaction effect. Arrows indicate bands of interest.

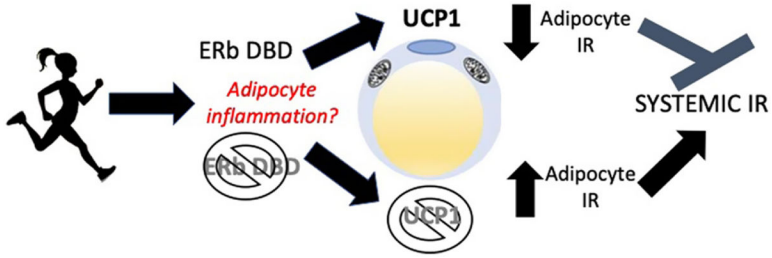

Figure 8.

The hypothesized mechanism of the exercise-induced increase in insulin resistance (IR) in ERbDBDKO mice. Exercise increases mitochondrial activity, which associates with increased reactive oxygen species (ROS) and inflammation. UCP1 is an insulin-sensitizing protein that is often upregulated by exercise in adipose tissue for reasons that are not clear and via mechanisms that are not fully known. We propose that UCP1 upregulation is protective against adipocyte stress (e.g. exercise) and buffers exercise-induced stress. Further, when exercise is not coupled with an appropriate increase in UCP1, as seen in these mutant mice lacking the ERb DBD, exercise-induced adipose tissue cell stress leads to increased adipocyte and systemic IR. A full color version of this figure is available at https://doi.org/10.1530/JOE-21–0009.

Table 1

qRT-PCR primer sequences.

	5′-3′ primer sequence forward	5′-3′ primer sequence reverse	Product length	NCBI reference sequence
TNFa	CTATGTCTCAGCCTCTTCTC	CATTTGGGAACTTCTCATCC	109 bp	NM_013693.3
Adiponectin	GCACTGGCAAGTTCTACTGCAA	GTAGGTGAAGAGAACGGCCTTGT	122 bp	NM_009605.5
Leptin	CCTATTGATGGGTCTGCCCA	TGAGCGCTACCTGCATAGAC	95 bp	NM_008493.3
Beta actin	GATGTATGAAGGCTTTGGTC	TGTGCACTTTTATTGGTCTC	96 bp	NM_007393.5
F4/80	GTGCCATCATTGCGGGATTC	GACGGTTGAGCAGACAGTGA	555 bp	X93328.1
PGC1a	CCCTGCCATTGTTAAGACC	TGCTGCTGTTCCTGTTTTC	161 bp	NM_008904.2
GPX3	GTATGGAGCCCTCACCATCG	GCTCTTTCTCCCCGTTCACA	407 bp	NM_001329860.1
COX IV	GTATCAGAGGGGGTGCACAA	GACTGTGAGGTCACATGGCT	134 bp	AF500216.1
GRP75	TGATTGGAATTCCCCCAGCC	TGCACTGCCACGATTACTGT	540 bp	NM_010481.2
UCP1	CACGGGGACCTACAATGCTT	ACAGTAAATGGCAGGGGACG	191 bp	NM_009463.3
ERa	CAAGGTAAATGTGTGGAAGG	GTGTACACTCCGGAATTAAG	140 bp	NM_007956.5
ERb	CTCAACTCCAGTATGTACCC	CATGAGAAAGAAGCATCAGG	178 bp	NM_010157.3
ERb DBD	TGTTACTAGTCCAAGCGCCAA	CATCCTTCACAGGACCAGACA	99 bp	NM_010157.3
PPARg	CGGGCTGAGAAGTCACGTT	TGCGAGTGGTCTTCCATCAC	200 bp	NM_001127330.2

J Endocrinol. Author manuscript; available in PMC 2022 May 24.

Table 2

Western blot antibodies.

Protein	Supplier
Adiponectin	Cell Signaling 2789
ERa	Abcam 75635
ERb	Abcam 3577
MCP1	Cell Signaling 2029
NFkB	Cell Signaling 4764
TNFa	Abcam 106606
UCP1	Sigma U6382
Total OxPhos Cocktail	Abcam 110413

Table 3

Markers of body composition, adipocyte size, and final tissue weights.

	WT Sed	WT Ex	KO Sed	KO Ex	G, *P*-value	T, *P*-value	G×T, *P*-value
SQAT (g)	1.1 ± 0.12	1.2 ± 0.05	1.1 ± 0.13	1.0 ± 0.16	0.453	0.945	0.424
PGAT (g)	2.0 ± 0.16	2.2 ± 0.10	2.0 ± 0.26	2.0 ± 0.29	0.737	0.685	0.612
Liver (g)	1.2 ± 0.09	1.3 ± 0.05	1.3 ± 0.09	1.3 ± 0.12	0.573	0.473	0.992
BAT (g)	0.07 ± 0.00	0.07 ± 0.00	0.08 ± 0.01	0.08 ± 0.01	0.245	0.398	0.494
Lean mass (% BW)	57.6 ± 2.23	56.5 ± 1.60	60.1 ± 2.64	61.4 ± 2.84	0.128	0.978	0.612
Fat mass (% BW)	38.2 ± 2.49	39.7 ± 1.05	37.4 ± 3.24	35.1 ± 3.28	0.311	0.872	0.481
Total lean mass (g)	19.1 ± 0.37	19.6 ± 0.30	19.7 ± 0.29	20.2 ± 0.38	0.098	0.112	0.981
Total fat mass (g)	13.2 ± 1.20	13.9 ± 0.66	12.8 ± 1.48	12.4 ± 1.77	0.468	0.920	0.656
Average PGAT cell size per 50 cells (μm)	4400.8 ± 859.18	3518.7 ± 562.40	6019.0 ± 887.66	3811.4 ± 438.99	0.217	0.062	0.380

For PGAT adipocyte size, 50 adipocytes were assessed/animal; $n = 3$/group. Unless otherwise indicated, $n = 10–11$/group. $P \leq 0.05$ was considered significant.

BAT, interscapular brown adipose tissue; G, genotype effect; G×T, genotype × treatment interaction effect; PGAT, perigonadal white adipose tissue; SQAT, inguinal s.c. white adipose tissue; T, treatment effect.

Table 4

Fasting blood biochemistry.

	WT Sed	WT Ex	KO Sed	KO Ex	G, *P*-value	T, *P*-value	G×T, *P*-value
Estradiol (pg/mL)	5.10 ± 0.91	4.69 ± 0.79	4.10 ± 0.62	4.92 ± 0.95	0.649	0.809	0.467
NEFA (mmol/L)	0.27 ± 0.01	0.26 ± 0.02	0.31 ± 0.02	0.28 ± 0.02	0.066	0.368	0.543
Insulin (ng/mL)	0.61 ± 0.13	0.67 ± 0.07	0.59 ± 0.09	1.12 ± 0.18	0.092	**0.027** *	0.076
Glucose (mg/dL)	238.5 ± 12.9	217.1 ± 13.1	241.4 ± 18.0	236.2 ± 15.3	0.468	0.382	0.593

Plasma was collected at sacrifice 8 weeks following OVX. n = 10–11/group. $P \leq 0.05$ was considered significant and designated by *.

G, genotype effect; G×T, genotype × treatment interaction effect; NEFA, non-esterified fatty acids; T, treatment effect.